STRUCTURAL BIOLOGY

ISSN: 2059-7983
journals.iucr.org/d

Structures of the apo and holo forms of formate dehydrogenase from the bacterium *Moraxella* sp. C-1: towards understanding the mechanism of the closure of the interdomain cleft

I. G. Shabalin, E. V. Filippova, K. M. Polyakov, E. G. Sadykhov, T. N. Safonova, T. V. Tikhonova, V. I. Tishkov and V. O. Popov

Acta Cryst. (2009). D**65**, 1315–1325

Acta Crystallographica Section D
Biological Crystallography
ISSN 0907-4449

Structures of the apo and holo forms of formate dehydrogenase from the bacterium *Moraxella* sp. C-1: towards understanding the mechanism of the closure of the interdomain cleft

I. G. Shabalin,[a] E. V. Filippova,[b]‡ K. M. Polyakov,[a,b] E. G. Sadykhov,[a] T. N. Safonova,[a] T. V. Tikhonova,[a] V. I. Tishkov[a,c] and V. O. Popov[a]*

[a]A. N. Bach Institute of Biochemistry, Russian Academy of Sciences, Leninsky Prospect 33, Moscow 119071, Russia, [b]Engelhardt Institute of Molecular Biology, Russian Academy of Sciences, Vavilova Street 32, Moscow 119991, Russia, and [c]Department of Chemical Enzymology, Faculty of Chemistry, M. V. Lomonosov Moscow State University, Leninskie Gory, Moscow 119992, Russia

‡ Present address: Department of Molecular Pharmacology and Biological Chemistry, Northwestern University, Feinberg School of Medicine, Chicago, Illinois 60611, USA.

Correspondence e-mail: vpopov@inbi.ras.ru

Received 2 July 2009
Accepted 6 October 2009

PDB References: holo MorFDH, 2gsd, r2gsdsf; apo MorFDH, 3fn4, r3fn4sf.

NAD$^+$-dependent formate dehydrogenase (FDH) catalyzes the oxidation of formate ion to carbon dioxide coupled with the reduction of NAD$^+$ to NADH. The crystal structures of the apo and holo forms of FDH from the methylotrophic bacterium *Moraxella* sp. C-1 (MorFDH) are reported at 1.96 and 1.95 Å resolution, respectively. MorFDH is similar to the previously studied FDH from the bacterium *Pseudomonas* sp. 101 in overall structure, cofactor-binding mode and active-site architecture, but differs in that the eight-residue-longer C-terminal fragment is visible in the electron-density maps of MorFDH. MorFDH also differs in the organization of the dimer interface. The holo MorFDH structure supports the earlier hypothesis that the catalytic residue His332 can form a hydrogen bond to both the substrate and the transition state. Apo MorFDH has a closed conformation of the interdomain cleft, which is unique for an apo form of an NAD$^+$-dependent dehydrogenase. A comparison of the structures of bacterial FDH in open and closed conformations allows the differentiation of the conformational changes associated with cofactor binding and domain motion and provides insights into the mechanism of the closure of the interdomain cleft in FDH. The C-terminal residues 374–399 and the substrate (formate ion) or inhibitor (azide ion) binding are shown to play an essential role in the transition from the open to the closed conformation.

1. Introduction

NAD$^+$-dependent formate dehydrogenase (EC 1.2.1.2; FDH) oxidizes the formate ion to carbon dioxide coupled with the reduction of NAD$^+$ to NADH. The enzyme belongs to a family of D-isomer-specific 2-hydroxyacid dehydrogenases (Vinals *et al.*, 1993), is rather abundant and plays an important role in the energy supply of methylotrophic microorganisms and in the stress response in plants (Tishkov & Popov, 2004).

FDH is a well studied protein that has been described in a number of reviews, the most recent being Tishkov & Popov (2004). The catalytic mechanism of the enzyme involves a direct hydride-ion transfer from the substrate with a relatively simple structure to the C4 atom of the nicotinamide moiety of NAD$^+$ and is devoid of proton-transfer steps (Popov & Tishkov, 2003). Because of this apparent simplicity, FDH has been widely accepted as a model for study of the mechanism of hydride-ion transfer in the active centre of NAD$^+$-dependent dehydrogenases (Castillo *et al.*, 2008; Bandaria *et al.*, 2008; Torres *et al.*, 1999).

FDH has a number of important practical applications. The enzyme is widely used for NAD(P)H regeneration in the enzymatic synthesis of chiral compounds with NAD$^+$-dependent dehydrogenases (Weckbecker & Hummel, 2004;

Ernst *et al.*, 2005). Owing to the irreversibility of the enzymatic reaction and the wide pH optimum of its activity, the enzyme is a versatile biocatalyst for many chemical processes. Bacterial FDHs have advantages over FDHs from other organisms in practical applications as they have been found to be more efficient in terms of activity and stability (Tishkov & Popov, 2006).

FDH crystal structures have been solved for two species: the methylotrophic bacterium *Pseudomonas* sp. 101 (PseFDH) and the yeast *Candida boidinii* (CboFDH). Consequently, the structures of two crystallographic modifications of apo PseFDH (Lamzin *et al.*, 1994; Filippova *et al.*, 2005), the structures of two complexes of PseFDH with the formate ion (Filippova *et al.*, 2006), the structure of holo PseFDH as a ternary complex with NAD^+ and the azide ion (Lamzin *et al.*, 1994) and the structures of two apo CboFDH mutants (Schirwitz *et al.*, 2007) have been reported.

The crystal structures, supported by biochemical studies, showed that FDH invariably exists as a homodimer, with two subunits being related by a twofold rotation axis. Each subunit of FDH consists of two domains: the internal coenzyme-binding domain and the peripheral catalytic domain. Each domain displays the same Rossmann-fold topology and exhibits high structural homology. The enzyme active site is located in a deep cleft that separates the two domains. The cofactor is bound in the cleft; the active site is accessible to the bulk solvent through a long and wide substrate channel (Popov & Lamzin, 1994; Schirwitz *et al.*, 2007).

Like many other NAD^+-dependent dehydrogenases, FDH can exist in so-called 'open' and 'closed' conformational states. Transition from the open to the closed conformation is essential for the formation of the enzyme active site and for catalysis. This transition in PseFDH is accomplished *via* a rotation of the peripheral catalytic domains by 7.5° around two domain-connecting hinges towards the respective coenzyme-binding domains and is accompanied by structuring of the protein C-terminus (residues 374–391) and formation of the C-terminal α-helix (Lamzin *et al.*, 1994).

Only one crystal structure of FDH (holo PseFDH) in the closed conformation has been described previously. In the present study, we report the structures of a novel FDH from the methylotrophic bacterium *Moraxella* sp. C-1 (MorFDH) in the apo and holo (ternary complex with NAD^+ and the azide ion) forms at 1.96 and 1.95 Å resolution, respectively. Both structures have the closed conformation of the interdomain cleft, with apo MorFDH being a rare example of an apo NAD^+-dependent dehydrogenase trapped in the closed conformation. We report a comparison of the MorFDH and PseFDH structures, giving insights into the mechanism of closure of the interdomain cleft in FDH.

2. Experimental

2.1. Expression, purification and enzyme characterization

Recombinant full-length (401 amino-acid residues according to the gene sequence) MorFDH was obtained by expression in *Escherichia coli* cells. The pPseFDH6a plasmid (Tishkov *et al.*, 1999) was used for construction of the expression vector for MorFDH. In the pPseFDH6a plasmid, the PseFDH gene is cloned under the control of tandem *lac* and *tac* promoters using *Nde*I and *Eco*RI restriction sites. The *Nde*I and *Eco*RI restriction-endonuclease sites were introduced at the beginning and end of the MorFDH gene by PCR using the following primers (restriction sites are shown in bold): forward, 5′-G **ACC ATG G**CC AAG GTT GTT TGC G-3′; reverse, 5′-CT**G AAT TC**A GGC GTC GAG CTT TTC GTA TTT CGC-3′.

The PCR product and pPseFDH6a plasmid were digested by *Nde*I and *Eco*RI, purified in agarose gel and ligated to produce the pMxFDH8a expression vector. *E. coli* TG1 cells were then transformed by the ligation product. Two of four colonies were taken to purify the pMxFDH8a plasmid using a QIAprep Spin Miniprep Kit (Qiagen). The plasmids were sequenced with an ABI PRISM 3100-Avant automated DNA Sequencer (Applied Biosystems) to prove the absence of mutations in the MorFDH gene.

E. coli cells containing recombinant MorFDH were produced by the cultivation of a single colony in 200 ml 2YT medium (16 g l^{-1} Bacto tryptone and 10 g l^{-1} yeast extract, both from Difco, USA) and 10 g l^{-1} NaCl pH 7.0 containing 150 µg ml^{-1} ampicillin for 12–15 h at 310 K. To induce MorFDH biosynthesis, isopropyl β-D-1-thiogalactopyranoside (IPTG) was added to 0.5 m*M* at the beginning of cultivation. The cells were collected by centrifugation in a Beckman J-21 centrifuge (USA) at 8000*g* for 10 min. Further purification of MorFDH was performed using the standard protocol developed for recombinant PseFDH expressed in *E. coli* (Tishkov *et al.*, 1999). The protocol included cell disruption in an ultrasonic disintegrator, ammonium sulfate fractionation (40% saturation) and FPLC hydrophobic interaction chromatography (Pharmacia Biotech, Sweden) on a 1 × 10 cm column packed with highly substituted Phenyl Sepharose Fast Flow (Pharmacia Biotech) followed by gel filtration using Sephacryl S-200 Superfine (2.5 × 90 cm column; Pharmacia Biotech).

The purity of the recombinant enzyme was at least 95% (from analytical SDS–PAGE). The MorFDH activity was determined spectrophotometrically by measuring the accumulation of NADH at 340 nm (ε_{340} = 6220 M^{-1} cm^{-1}) on a Shimadzu UV 1601PC spectrophotometer (Japan) at 303 K in 0.1 *M* potassium phosphate buffer pH 7.0. The concentrations of NAD^+ and sodium formate in the cell were 1.5 m*M* and 0.3 *M*, respectively. The catalytic characteristics of recombinant full-length MorFDH and PseFDH are compared in Table 1.

Table 1
Catalytic characteristics of recombinant full-length MorFDH and PseFDH (303 K, pH 7.0).

The data for PseFDH are from Tishkov *et al.* (1996).

Enzyme	k_{cat} (s^{-1})	K_m for formate (m*M*)	K_m for NAD^+ (µ*M*)
MorFDH	7.3 ± 0.4	7.7 ± 0.4	80 ± 3
PseFDH	7.3 ± 0.5	8.0 ± 0.4	65 ± 2

2.2. Crystallization

All crystallization experiments were performed by the hanging-drop vapour-diffusion method using 24-well plates with a 500 µl reservoir volume at room temperature. Hampton Research protein-crystallization kits were used for initial crystallization screening and the crystallization conditions were then optimized.

The best crystals of holo MorFDH were grown in hanging drops containing 1 µl protein solution and 1 µl reservoir solution. The protein solution was composed of 11 mg ml^{-1} MorFDH in 0.1 *M* K_2HPO_4 buffer pH 7.0, 5 m*M* NAD^+ and 5 m*M* sodium azide. The reservoir solution was composed of 2.3 *M* ammonium sulfate in 0.1 *M* bis-tris buffer pH 6.5. Colourless crystals grew to average dimensions of approximately 0.5 × 0.3 × 0.2 mm within one week.

The best crystals of apo MorFDH were grown in hanging drops containing 1 µl protein solution and 1 µl reservoir solution. The protein solution contained 10.5 mg ml^{-1} MorFDH in 0.1 *M* Na_2HPO_4 buffer pH 7.0. The reservoir solution contained 2.2 *M* ammonium sulfate and 2% PEG 400 in 0.1 *M* HEPES buffer pH 7.5. Colourless crystals grew to average dimensions of approximately 0.6 × 0.2 × 0.2 mm within one week.

2.3. Data collection, structure determination and refinement

The X-ray diffraction data set for holo MorFDH was collected at room temperature from a single crystal using a MAR 345 image-plate detector on an Elliott GX-6 rotating-anode generator at the Institute of Protein Research of the Russian Academy of Sciences (Pushino, Moscow Region, Russia). The X-ray data were indexed, integrated, scaled and merged with the *XDS* software package (Kabsch, 1993). The crystals belonged to space group *C*2, with unit-cell parameters $a = 80.45$, $b = 66.5$, $c = 75.55$ Å, $\beta = 103.57^\circ$.

The X-ray diffraction data set for apo MorFDH was collected from a single crystal at 100 K in a nitrogen stream using a MAR CCD 165 mm detector on the K4.4 beamline at the Kurchatov Center for Synchrotron Radiation and Nanotechnology (Moscow, Russia). Prior to flash-freezing, the crystal was soaked in cryoprotectant [0.1 *M* HEPES buffer pH 7.5, 2.2 *M* ammonium sulfate and 20%(*v*/*v*) glycerol] for approximately 5 min. The data were indexed, integrated, scaled and merged with the *AUTOMAR* program suite (Klein & Bartels, 2000). The crystals belonged to space group *C*2, with unit-cell parameters $a = 80.66$, $b = 66.09$, $c = 75.55$ Å, $\beta = 104.13^\circ$.

The structure of holo MorFDH was solved by the molecular-replacement method using the *MOLREP* program (Vagin & Teplyakov, 1997). The structure of the FDH subunit of holo PseFDH (PDB code 2nad; Lamzin *et al.*, 1994) was used as the starting model. Since the crystals of the apo and holo forms of the enzyme were isomorphous, the structure of holo MorFDH (without the cofactor) was used as the starting model for the refinement of apo MorFDH.

The structures were refined with the *REFMAC* program (Murshudov *et al.*, 1997) in the restrained mode. The graphics program *Coot* (Emsley & Cowtan, 2004) was used for the visualization of electron-density maps, rebuilding of atomic models and addition of water molecules. The quality of the models was inspected using the program *PROCHECK* (Laskowski *et al.*, 1993). The data-collection and refinement statistics are given in Table 2.

Table 2
Data-collection and refinement statistics.

Values in parentheses are for the highest resolution shell.

	Holo MorFDH	Apo MorFDH
Data-collection statistics		
Wavelength (Å)	1.54	1.05
Resolution range (Å)	27.8–1.95 (2.00–1.95)	39.1–1.96 (2.05–1.96)
No. of observed reflections	67848	88327
No. of unique reflections	27554	27648
Mosaicity (°)	0.35	0.7
$R_{merge}(I)$ (%)	9.4 (35.7)	12.2 (47.6)
Completeness (%)	97.1 (95.1)	99.5 (100)
Redundancy	2.5 (2.4)	3.3 (3.3)
$I/\sigma(I)$	8.0 (3.0)	6.0 (2.1)
B factor from Wilson plot (Å^2)	25.7	33.1
Matthews coefficient (Å^3 Da^{-1})	2.23	2.24
Refinement statistics		
Resolution range (Å)	73.52–1.95	73.32–1.96
No. of reflections used	26730	26255
Size of R_{free} set (%)	5	5
R_{work} (%)	14.2	18.7
R_{free} (%)	18.4	24.0
R.m.s. deviation from ideal		
Bonds (Å)	0.018	0.020
Angles (°)	1.619	1.820
Ramachandran plot, residues in		
Most favoured regions (%)	89.4	86.4
Additional allowed regions (%)	10.3	13.3
Disallowed regions (%)	0.3†	0.3†
Luzzati coordinate error (Å)	0.169	0.223
No. of non-H atoms		
Protein	3097	3005
Water	181	97
Ligands	47	12
Average *B* factors (Å^2)		
Protein	18.6	32.4
Water	27.4	33.1
Ligands	12.6	30.1

† Ala198 is outside the allowed region.

2.4. Structure analysis

The structures were analyzed using *Coot, CCP*4*MG* (Potterton *et al.*, 2004), *CONTACT* and other programs from the *CCP*4 suite (Collaborative Computational Project, Number 4, 1994). The *ClustalW* program was used for sequence alignment (Larkin *et al.*, 2007). The dimer interface and crystal contacts were analyzed using the *PISA* service at the European Bioinformatics Institute (Krissinel & Henrick, 2007) and the *CONTACT* program. The secondary structure was determined with the *DSSP* program (Kabsch & Sander, 1983). Figs. 1, 3 and 5–8 were generated using *CCP*4*MG*; Fig. 4 was generated using *ISIS/Draw* 2.4. Hydrogen bonds at the active site and the pyrophosphate-binding subsite were assigned based on the commonly accepted geometrical criteria (donor–acceptor distance cutoff of 3.50 Å, *D*—H—*A* angle

cutoff of 120°) and verified visually accounting for the H-atom positions and the molecular geometry of the acceptor atoms.

3. Results and discussion

3.1. Overall structure of MorFDH

A ribbon representation of the MorFDH polypeptide chain is shown in Fig. 1 for the holo form. The crystal structures of both apo and holo MorFDH contain one protein subunit per asymmetric unit. The subunits of the MorFDH dimer are related to each other by a crystallographic twofold rotation axis, as was observed for apo PseFDH crystallized in a tetragonal space group (Filippova *et al.*, 2005). The coenzyme-binding domain of MorFDH is formed by residues 147–333. The catalytic domain consists of residues 1–146 and 334–399. In both structures the last two C-terminal residues (400–401) are not visible in the electron-density maps.

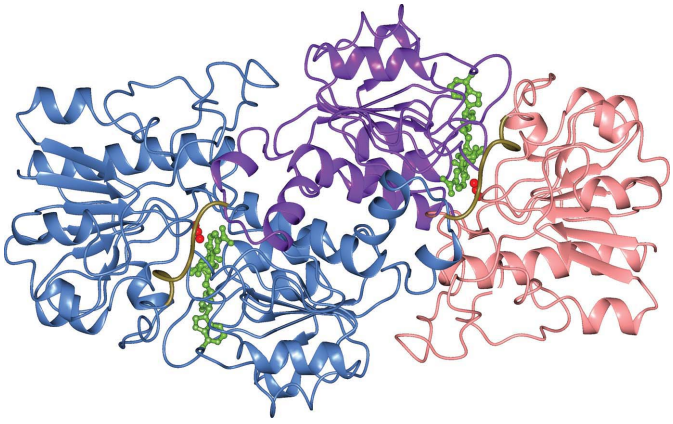

Figure 1
Ribbon representation of the holo MorFDH dimer. The crystallographic twofold rotation axis is perpendicular to the plane of the figure. The left monomer is coloured light blue. The coenzyme-binding and catalytic domains of the right monomer are represented in purple and pink, respectively. The NAD^+ and azide molecules are represented as ball-and-stick models in green and red, respectively. The eight extra C-terminal residues compared with the PseFDH structure are shown in dark olive green as a worm model for both subunits.

Both apo and holo MorFDH were obtained in the closed conformation. Apo and holo MorFDH resemble each other very closely and can be superimposed with an r.m.s. deviation of 0.31 Å for all C^α atoms. Only the C^α atoms in the binding region of the adenine moiety of the cofactor (residues 222–224) show deviations of greater than 1 Å.

MorFDH displays 85.5% sequence identity to PseFDH and differs from the latter at 58 residues (Fig. 2). MorFDH and PseFDH have nearly identical secondary structures. Their holo forms can be superimposed with an r.m.s. deviation of 0.42 Å for all 391 C^α atoms present in the holo PseFDH structure. R.m.s. deviations greater than 1.0 Å are only observed for C^α atoms in the catalytic domain (residues 17, 67, 79, 87–88 and 112); the maximum deviation is less than 1.7 Å (residue 17). A separate pairwise comparison of the individual domains for the holo forms of MorFDH and PseFDH gives r.m.s. deviations of 0.34 and 0.41 Å for the C^α atoms of the coenzyme-binding and catalytic domains, respectively. Hence, the coenzyme-binding domain is structurally more conserved than the catalytic domain in the bacterial FDHs under consideration.

MorFDH has a deep substrate channel leading from the protein surface to the enzyme active site. The substrate channel in MorFDH is very similar to that in PseFDH, the spatial organization of which has been described previously (Lamzin *et al.*, 1994). The entrance to the channel in both MorFDH structures is covered by the loop 385–390, as in holo

```
                  β1                                                                                  α1
MorFDH    1 AKVVCVLYDDPINGYPTSYARDDLPRIDKYPDGQTLPTPKAIDFTPGALLGSVSGELGLR 60
PseFDH    1 AKVLCVLYDDPVDGYPKTYARDDLPKIDHYPGGQTLPTPKAIDFTPGQLLGSVSGELGLR 60
            α2          β2                    α3          β3                    α4          β4
MorFDH   61 KYLESQGHELVVTSSKDGPDSELEKHLHDAEVIISQPFWPAYLTAERIAKAPKLKLALTA 120
PseFDH   61 KYLESNGHTLVVTSDKDGPDSVFERELVDADVVISQPFWPAYLTPERIAKAKNLKLALTA 120
                        α5          β5                    α6          α7
MorFDH  121 GIGSDHVDLQAAIDNNITVAEVTYCNSNSVAEHVVMMVLGLVRNYIPSHDWARNGGWNIA 180
PseFDH  121 GIGSDHVDLQSAIDRNVTVAEVTYCNSISVAEHVVMMILSLVRNYLPSHEWARKGGWNIA 180
            α8                β6                    α9          β7                    α10         β8
MorFDH  181 DCVARSYDVEGMHVGTVAAGRIGLRVLRLLAPFDMHLHYTDRHRLPEAVEKELNLTWHAT 240
PseFDH  181 DCVSHAYDLEAMHVGTVAAGRIGLAVLRRLAPFDVHLHYTDRHRLPESVEKELNLTWHAT 240
            α11         β9                    α12         β10         α13         α14
MorFDH  241 REDMYGACDVVTLNCPLHPETEHMINDETLKLFKRGAYLVNTARGKLCDRDAIVRALESG 300
PseFDH  241 REDMYPVCDVVTLNCPLHPETEHMINDETLKLFKRGAYIVNTARGKLCDRDAVARALESG 300
                  β11                   α15                   α16         α17
MorFDH  301 RLAGYAGDVWFPQPAPNDHPWRTMPHNGMTPHISGTSLSAQTRYAAGTREILECYFEGRP 360
PseFDH  301 RLAGYAGDVWFPQPAPKDHPWRTMPYNGMTPHISGTTLTAQARYAAGTREILECFFEGRP 360
              α18  β12     β13   α19                   α20
MorFDH  361 IRDEYLIVQGGGLAGVGAHSYSKGNATGGSEEAAKYEKLDA                    401
PseFDH  361 IRDEYLIVQGGALAGTGAHSYSKGNATGGSEEAAKFKKAV-                    400
```

Figure 2
Alignment of the full-length MorFDH and PseFDH amino-acid sequences (UniProt references O08375 and P33160, respectively). The secondary-structure elements are shown for the holo forms. The residues involved in the dimer interface in the respective holo forms are shown on a green background.

Table 3
Additional crystallographically non-equivalent hydrogen bonds involved in the dimer interface in holo MorFDH.

The corresponding residues in PseFDH are given in parentheses.

Monomer *A*		Monomer *B*		
Residue	Atom	Residue	Atom	Distance (Å)
Asn148 (Ile)	ND2	Glu190 (Glu)	OE2	3.2
Asp170 (Glu)	OD1	Arg173 (Arg)	NH2	3.1
Asp170 (Glu)	OD2	Arg173 (Arg)	NH1	3.1
Arg205 (Ala)	NH1	Asp214 (Asp)	OD2	2.8
Arg205 (Ala)	NH2	Asp214 (Asp)	OD2	2.9
Asn317 (Lys)	ND2	Gly175 (Gly)	O	2.9

PseFDH. All eight water molecules found in the channel occupy similar positions in all known FDH structures that have a closed interdomain cleft (apo MorFDH, holo MorFDH and holo PseFDH). This fact confirms the hypothesis that the substrate channel is highly conserved and functionally significant (Popov & Tishkov, 2003).

In both MorFDH structures the residue Ala198 is outside the allowed region of the Ramachandran plot. The residues Pro312 and Pro314 in these structures are in the *cis* conformation. These structural features are the same as in PseFDH and their implications for catalysis have been described previously (Lamzin *et al.*, 1994).

3.2. C-terminal fragment 392–399

In the apo and holo MorFDH structures extra C-terminal residues 392–399 (compared with PseFDH; Fig. 1) were observed in the electron-density maps, whereas only residues 1–374 and 1–391 were located in the apo and holo PseFDH structures, respectively. The larger number of residues in holo PseFDH compared with apo PseFDH was accounted for by the structuring of the C-terminal residues upon transition from the open to the closed conformation (Lamzin *et al.*, 1994). In the holo PseFDH structure the nine last C-terminal residues were not observed, which may be attributed to their disorder or enzyme proteolysis in the initial strain *Pseudomonas* sp. 101. As shown previously, native PseFDH exists as several isoforms (Tishkov *et al.*, 1991). This was assigned as arising from partial proteolysis of the C-terminus by up to seven residues, with a resulting decrease in the affinity of PseFDH for formate by a factor of two. Attempts to determine the crystal structure of full-length PseFDH have failed, apparently owing to the fact that the C-terminal residues may hinder crystallization. In the present study, we have established the structures of recombinant full-length MorFDH, the catalytic properties of which are similar to those of recombinant full-length PseFDH (Table 1).

The extra C-terminal fragment 392–399 found in the MorFDH structures belongs to the catalytic domain. Spatially, it is located between the catalytic domain core and the coenzyme-binding domain and shields the interdomain cleft (Figs. 1 and 3). The presence of the extra C-terminal residues results in the formation of α-helix 390–395 (α20) that is absent from the holo PseFDH structure (Fig. 2). The main-chain O and N atoms of the C-terminal residue Glu397 form two hydrogen bonds to the side-chain atoms OD1 and ND2 of Asn317 from the coenzyme-binding domain. The C-terminal residue Tyr396 is involved in a hydrophobic cluster with Pro314 from the coenzyme-binding domain, Trp99 from the catalytic domain and Trp177 from the coenzyme-binding domain of the adjacent subunit of the dimer (Fig. 3). Hence, the C-terminal fragment 392–399 is involved in several interactions with the coenzyme-binding domains of the dimer, thus contributing to interdomain interactions. This could be an important factor stabilizing the closed conformation of the interdomain cleft in the apo MorFDH crystal structure.

3.3. Dimer interface

The dimer interfaces in MorFDH and PseFDH are formed by equivalent amino-acid sequence regions (Fig. 2). The interface areas in the holo forms of MorFDH and PseFDH are also similar (3953 and 3799 Å^2, respectively). The difference in the surface area (154 Å^2) mainly arises from the involvement of the extra C-terminal residues 392–399 in the interface in the MorFDH structure (Fig. 3). The dimer interface in holo MorFDH comprises 54 hydrogen bonds (and 12 salt bridges), as opposed to 42 hydrogen bonds (and ten salt bridges) in holo PseFDH. Surprisingly, all the hydrogen bonds that are present in PseFDH are preserved in MorFDH. 12 extra hydrogen bonds at the interface in holo MorFDH are attributed to four amino-acid exchanges (compared with PseFDH): Ile148Asn, Glu170Asp, Ala205Arg and Lys317Asn (Table 3). Two of these mutations (Glu170Asp and Ala205Arg) result in the formation of four strong 'fork-to-fork' salt bridges in the holo MorFDH dimer. The dimer-interface

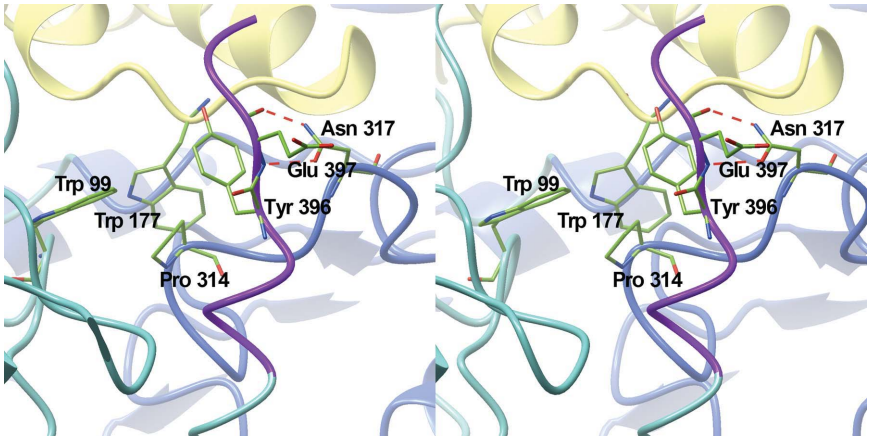

Figure 3
Stereoview of the extra C-terminal fragment 392–399 in holo MorFDH. The extra residues are shown in purple as a worm model. The catalytic domain core is depicted in cyan, the coenzyme-binding domain in blue and the coenzyme-binding domain of the adjacent subunit of the dimer in yellow. The interacting residues (see text for details) are shown in stick representation. Hydrogen bonds are shown as red dashed lines.

hydrophobicity can be evaluated as the solvation free-energy gain (without consideration of the effect of hydrogen bonding and salt-bridge formation) upon interface formation. This value, calculated using the *PISA* service at the European Bioinformatics Institute (Krissinel & Henrick, 2007), was -138 kJ mol^{-1} for holo MorFDH and -158 kJ mol^{-1} for holo PseFDH. Thus, the dimer interface in MorFDH is characterized by a larger number of hydrogen bonds and salt bridges but a lower hydrophobicity, with a nearly identical buried surface area.

These differences could lead to a considerable increase in the thermal stability of MorFDH as a result of optimization of electrostatic interactions (Li *et al.*, 2005; Folch *et al.*, 2007). For example, the rate of thermal inactivation of the Glu170Asp mutant of PseFDH is 20% lower than that of full-length PseFDH (Tishkov, 2009). However, a comparison of the DSC data shows that the melting point of MorFDH (336.4 K) is 4.5 K lower than that of PseFDH (Sadykhov *et al.*, 2006). However, as can be seen from the DSC curves, the thermal denaturation of MorFDH and PseFDH is a one-step highly cooperative process that does not implicate the dissociation of the enzyme molecules into subunits in intermediate steps. Thus, the nature of the dimer interface would not have a decisive impact on the thermal stability of the enzyme, since stabilizing interactions at the interface can be diminished by the differences in the amino-acid sequence in other fragments of the enzyme. Our data support this hypothesis in view of the fact that the less stable protein (MorFDH) has the greater dimer interface.

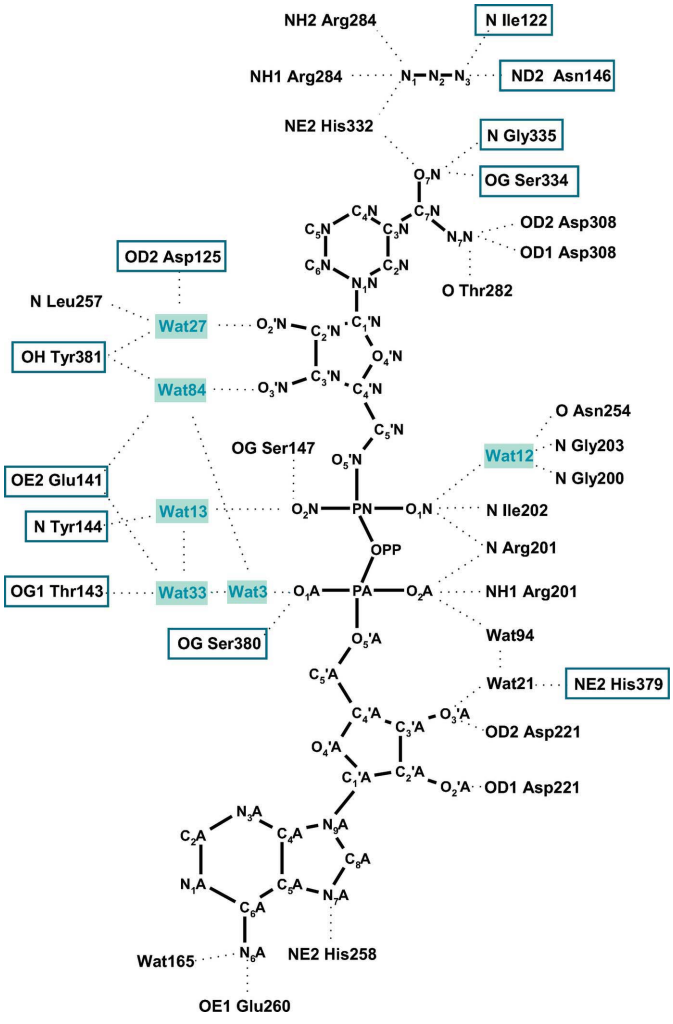

Figure 4
Scheme of NAD$^+$ and azide-ion binding in the active site of holo MorFDH. The catalytic domain residues are framed. Water molecules that are present in the structures of both apo and holo MorFDH are shown with blue shading.

3.4. Cofactor binding

In the holo MorFDH structure the whole NAD$^+$ molecule is clearly visible in the electron-density map. The cofactor binds in the cleft between two domains (Fig. 1) and mainly interacts with residues of the coenzyme-binding domain (Fig. 4). The cofactor-binding mode is the same as that observed in the holo PseFDH structure. The only difference from PseFDH is the absence of the water molecule in the vicinity of the N_1A atom of the cofactor. In holo PseFDH the cofactor is bound to Arg241 NH1 through this water molecule. Six of the nine water molecules involved in NAD$^+$ binding are preserved in the apo MorFDH crystal structure with the same hydrogen-bonding network (Fig. 4).

As can be seen from a comparison of the apo and holo MorFDH structures, NAD$^+$ binding causes conformational changes of the residues in the binding region of the adenine moiety of the cofactor. In this region, deviations of C^α atoms of greater than 0.5 Å are observed for residues 221–226, 259–260 and 379–383 (most of these residues are shown in Fig. 5), with the largest differences for these fragments of the polypeptide chain being 2.3 Å (His223), 0.6 Å (Glu260) and 0.8 Å (Tyr381), respectively. In apo MorFDH these three fragments are not hydrogen bonded to each other and the side chains of four residues (Arg222, Glu260, His379 and Ser382) are disordered and are not visible in the electron-density map. Moreover, no

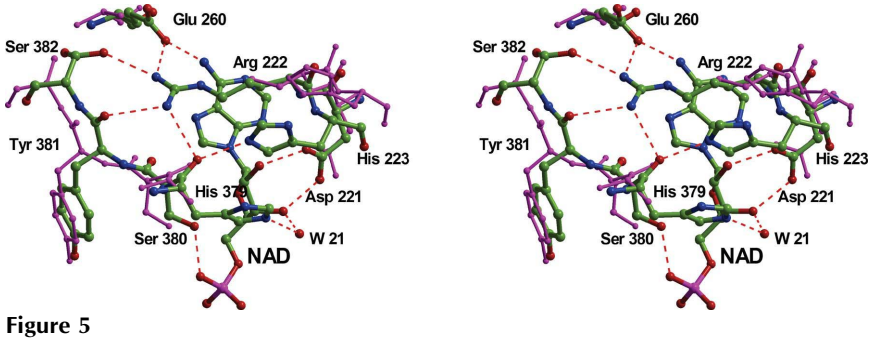

Figure 5
Stereoview of the adenine-binding subsite in apo and holo MorFDH. The residues and the NAD$^+$ molecule in holo MorFDH are coloured by atom type; apo MorFDH is shown in magenta. Hydrogen bonds are indicated by red dashed lines. The side chains of Arg222, Glu260, His379 and Ser382 in the apo MorFDH structure are disordered and are not visible in electron-density maps.

extra molecules were found in the adenine-binding subsite of apo MorFDH, suggesting that this large void space is filled with disordered water in the absence of NAD^+. In the holo MorFDH structure the cofactor forms five hydrogen bonds to the Asp221 (two bonds), Glu260, His379 (*via* water molecules) and Ser380 residues of these fragments, and the fragments are linked to each other by five direct hydrogen bonds. The hydrogen bonding results in movement of residues of these fragments into closer proximity to both each other and the cofactor molecule (Fig. 5).

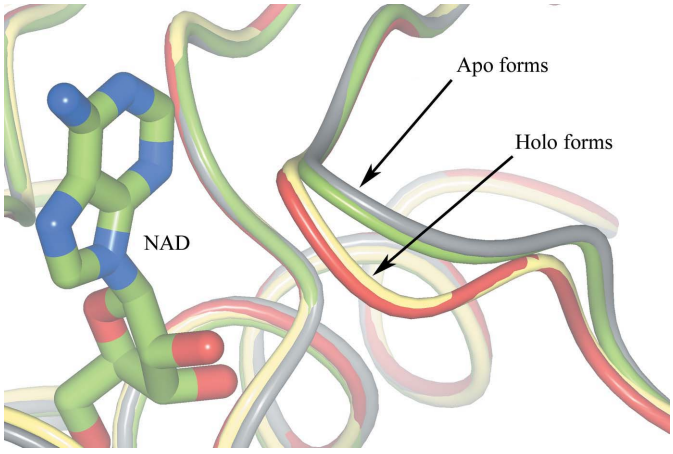

Figure 6
The difference in the arrangement of loop 221–226 in the apo and holo forms of MorFDH and PseFDH. Apo MorFDH is in grey and apo PseFDH is in green. Holo MorFDH is in red and holo PseFDH is in yellow. The superposition was performed by fitting the C^{α} atoms of the coenzyme-binding domains.

Loops 221–226 in apo and holo MorFDH are conformationally similar to those in apo and holo PseFDH, respectively (Fig. 6). It should be noted that this loop adopts the same conformation in the apo forms despite the fact that apo MorFDH is in the closed form, whereas apo PseFDH is in the open form. Hence, it can be hypothesized that the conformational changes in the 221–226 loop are fully induced by cofactor binding, whereas interdomain-cleft closure in the absence of the cofactor is not sufficient to cause these changes. It should be emphasized that the conformation of loop 221–226 in apo MorFDH remains the same as in apo PseFDH despite the fact that the C-terminal region 374–391 is structured, which could lead to the formation of four hydrogen bonds to residues 380–382 on the condition that the loop adopts the conformation that is observed in the holo form (Fig. 5).

In the apo MorFDH structure a sulfate ion and a water molecule (W57) are located in place of pyrophosphate in the coenzyme pyrophosphate-binding subsite. The same situation has been observed in the apo PseFDH structures (Filippova *et al.*, 2005; Lamzin *et al.*, 1994). The sulfate ion is mainly bound to the coenzyme-binding domain *via* direct interactions with Arg201 and Ile202 and *via* water-mediated contacts with Ser147, Gly200, Gly203 and Asn254 (Fig. 7). In addition, it forms hydrogen bonds *via* water molecules to the catalytic domain residues Glu141, Thr143 and Tyr144.

A comparison of the apo and holo forms of MorFDH and PseFDH shows that in all these structures water molecules W33 and W13 are in the same positions with respect to the catalytic domain, are bound to this domain by the same hydrogen bonds and move together with the catalytic domain upon transition from the open to the closed state. Hence, these water molecules can be assigned to the catalytic domain. Similarly, water molecules W3 and W57 can be assigned to the coenzyme-binding domain. The sulfate ion (SO4) can also be assigned to the coenzyme-binding domain because it is strongly bound to this domain by Coulombic interactions and hydrogen bonds. Hence, the domains in the apo MorFDH structure are linked together by four hydrogen bonds (*via* water molecules; W33···W3, W13···W3, W13···W57 and W13···SO4; see Fig. 7) in the pyrophosphate-binding subsite. In the apo-PseFDH structure with the open conformation the domains move apart from each other and there is only one hydrogen bond between the domains in this region (W13···W57). Since the sulfate ion in apo FDH enables more extensive hydrogen bonding between the domains in the closed conformation compared with the open conformation, the presence of sulfate ions in the crystallization medium may contribute to the stabilization of the closed conforma-

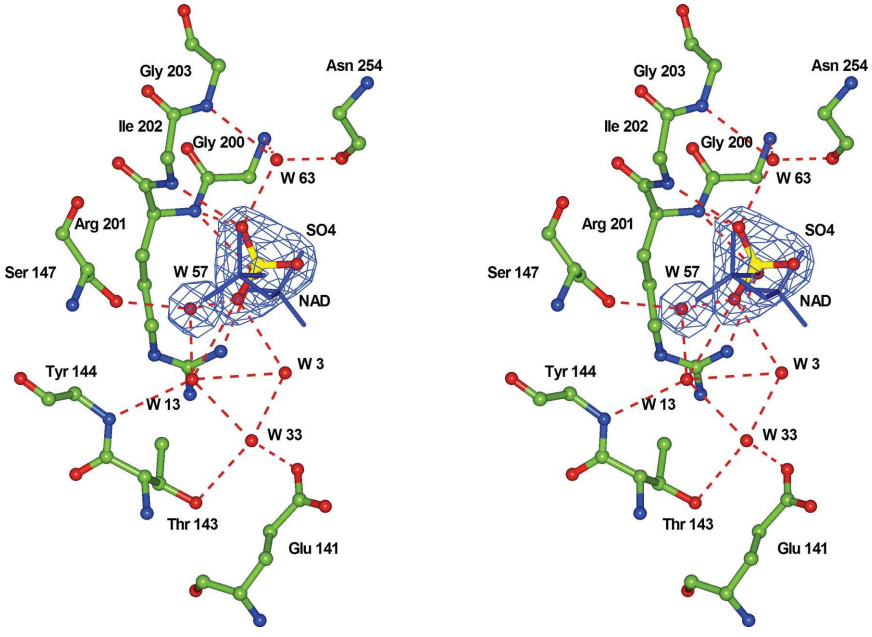

Figure 7
Stereoview of the pyrophosphate-binding subsite in apo MorFDH. Electron density contoured at the 1σ level is shown for the sulfate ion and water molecule W57. Hydrogen bonds are indicated by red dashed lines (for W13, all short contacts are shown). The pyrophosphate moiety of NAD^+ that is present in holo MorFDH is shown in a grey cylindrical representation after superimposition of the two structures by fitting all C^{α} atoms. The conserved water molecules are numbered in accordance with the holo MorFDH structure.

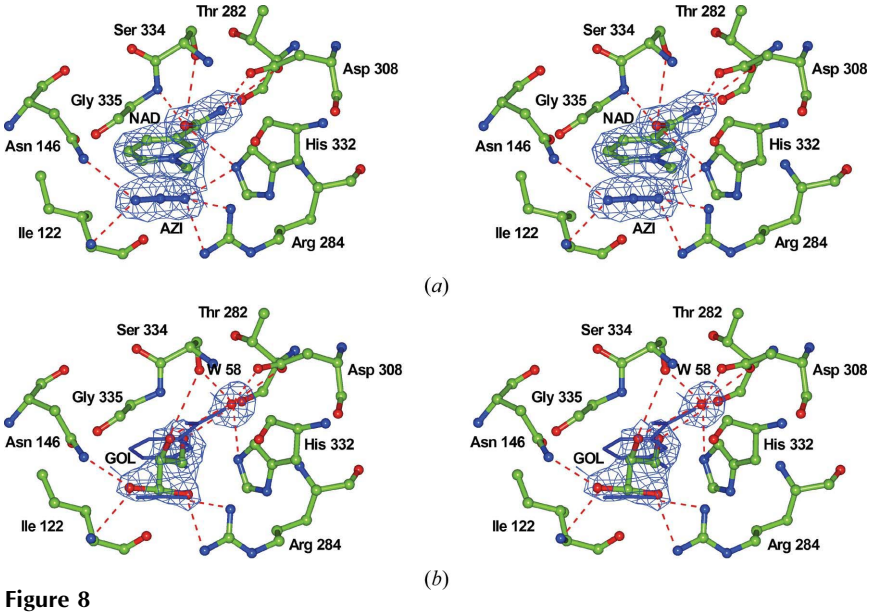

Figure 8
Stereoview of the catalytic site in holo MorFDH (*a*) and apo MorFDH (*b*). Hydrogen bonds are indicated by red dashed lines (for W58, all short contacts are shown). The electron density contoured at the 1σ level for the ligands. (*b*) The nicotinamide moiety of NAD^+ and the azide ion after superimposition of the two structures by fitting all C^α atoms are shown in blue cylindrical representations. One of the O atoms of the glycerol molecule has two positions. It is probable that one of the two positions can be assigned to a water molecule in 50% of the protein subunits that lack glycerol in the active site.

tion of apo MorFDH. As demonstrated by molecular-dynamics calculations for the related enzyme horse liver alcohol dehydrogenase, the interaction between the cofactor pyrophosphate and the coenzyme-binding domain plays a key role in bringing the domains closer together in the initial steps (Hayward & Kitao, 2006). Hence, it could be speculated that the negatively charged sulfate ion mimics and partially substitutes for the pyrophosphate moiety of the cofactor, thus enabling 'zipping' of the coenzyme-binding and catalytic domains of the protein.

3.5. Catalytic site

A stereoview of the MorFDH catalytic site is presented in Fig. 8. The catalytic sites of the MorFDH and PseFDH holo forms are quite similar. The main difference is that there is a hydrogen bond between the azide ion and the catalytic His332 residue in holo MorFDH. According to the proposed molecular mechanism of FDH (Popov & Tishkov, 2003), the azide ion occupies the same binding site as the substrate (the formate ion) and mimics the transition state of the enzymatic reaction. For PseFDH, site-directed mutagenesis experiments (Tishkov *et al.*, 1996) and molecular-dynamics studies (Torres *et al.*, 1999) showed that His332 is an essential residue for substrate binding and catalysis. However, the azide ion in the structure of holo PseFDH does not form a hydrogen bond to His332, as evidenced by the distance between the target atoms (3.6 Å). In the holo MorFDH structure this distance is 3.2 Å, thus allowing hydrogen bonding.

In apo MorFDH the catalytic site is occupied by a glycerol molecule (50% occupancy) and a water molecule, the position of which is identical to that of the N_7N atom of the cofactor (Fig. 8). We do not consider the glycerol molecule to be a possible factor contributing to the transition of apo MorFDH to the closed conformation, as glycerol was not used in the crystallization experiments and was only present in the cryoprotectant solution. Glycerol could diffuse into the protein crystals during soaking for approximately 5 min before flash-freezing and this is consistent with its 50% occupancy. It is hardly probable that the binding of glycerol would lead to the transition of the protein from the open to the closed conformation in the crystalline state because this transition occurs *via* the rotation of the peripheral catalytic domains by 7.5° around two domain-connecting hinges (Lamzin *et al.*, 1994). Such considerable structural changes should lead to crystal damage. Besides, glycerol is present in approximately one-half of the protein molecules. If glycerol were responsible for the transition from the open to the closed conformation, the protein would exist in the crystal structure both in the closed and open conformations since there is no glycerol in half of the protein molecules. To put it differently, all protein molecules could exist in the closed conformation only if glycerol had 100% occupancy.

It appears that the catalytic site was occupied by water molecules prior to the diffusion of glycerol because no other molecules or ions with appropriate sizes and charges (neutral or negative, since there is a positively charged Arg284 in the active site) that could occupy the active site in the closed conformation were present in the drop. Hence, we ruled out the possibility that binding of ligands in the active site could facilitate the transition of apo MorFDH to the closed conformation.

The catalytic site residues adopt nearly identical conformations in the apo and holo MorFDH structures (the deviations in the atomic positions are at most 0.6 Å), as opposed to the PseFDH structures, in which the catalytic site residues are significantly shifted in the apo form because of the open conformation of the enzyme (Lamzin *et al.*, 1994). Moreover, in apo PseFDH the catalytic site loop Ile122–Asp125 has two alternative conformations of the backbone (the maximum difference between the conformations being 2.9 Å for the main-chain atom O of Gly123) and the crucial catalytic site residue Arg284 has multiple conformations of the side chain (Filippova *et al.*, 2005, 2006), whereas in apo MorFDH these residues are fixed in a conformation similar to that of the holo form (Fig. 8). Additionally, binding of glycerol did not change the conformation of the active-site residues; otherwise, we would observe alternative conformations of these residues corresponding to the 50% of protein molecules containing glycerol in the active site. Hence, it can be stated that as a

result of the interdomain-cleft closure the catalytic site residues become structured and rigidly fixed in the catalytically competent conformation even without coenzyme binding.

3.6. Interdomain-cleft closure

The apo MorFDH structure is a rare example of an apo form of an NAD^+-dependent dehydrogenase with a closed conformation of the interdomain cleft. The crystallization of apo MorFDH in the closed conformation can be attributed to interactions of the extra C-terminal fragment 392–399 and sulfate-ion binding, since these two factors contribute to interdomain interactions and may be important for stabilization of the interdomain cleft in the closed conformation. It can also be speculated that the closed conformation is partly determined by crystal contacts, as the same contacts are present in isomorphous crystals of holo MorFDH, which also exists in the closed conformation, and in view of the fact that the crystallization conditions were similar for holo and apo MorFDH. One apo MorFDH subunit makes contacts with eight crystallographically related subunits (apart from the dimer interface), forming 20 hydrogen bonds and four salt bridges. The total interface surface area is 1576 $Å^2$, whereas the total solvent-accessible surface area is 13 310 $Å^2$ per monomer in the dimer. It is possible that these contacts could also contribute to the crystallization of apo MorFDH in the closed conformation.

Previously, it has been suggested that for some NAD^+-dependent dehydrogenases the energetic barrier between the open and the closed forms is rather low and these states can exist in a dynamic equilibrium (Kumar *et al.*, 1999; Razeto *et al.*, 2002; Stillman *et al.*, 1999). It appears that this hypothesis is also true for FDH because the enzyme conformation can be influenced by the presence of a few hydrogen bonds and hydrophobic interactions and possibly by several crystal contacts.

In the triple FDH–NAD^+–azide complex most of the hydrophobic interactions and the majority of hydrogen bonds between the cofactor and the enzyme are formed by residues from the coenzyme-binding domain (Fig. 4). However, the cofactor forms nine hydrogen bonds (six of them *via* water molecules) to the catalytic domain, acting as a bridge between the domains in the closed conformation. Thus, the cofactor plays a significant role in the transition from the open to the closed conformation.

The C-terminal residues 374–399 also play an essential role in the transition. The effect of residues 392–399 is discussed above. Residues 374–391 become structured upon closure of the interdomain cleft in PseFDH (Lamzin *et al.*, 1994). The importance of these residues is verified by the number of hydrogen bonds formed between the PseFDH domains in the two states. In the open conformation of apo PseFDH each catalytic domain forms 19 hydrogen bonds to the coenzyme-binding domains of the dimer. The transition to the closed state gives rise to 13 additional interdomain hydrogen bonds, seven of which are formed to the C-terminal fragment 374–391.

Binding of the cofactor facilitates the structuring of the C-terminal residues 374–399 because the cofactor forms hydrogen bonds to the C-terminal residues His379 (*via* the water molecule W21), Tyr381 (*via* the water molecules W27 and W84) and Ser380 (Figs. 4 and 5). In addition, cofactor binding causes a substantial shift of the loop 221–226 of the coenzyme-binding domain followed by the formation of four direct hydrogen bonds between this loop and the C-terminal residues 379–382 (Fig. 5). Apparently, these interactions of the cofactor play a significant role in the transition of the enzyme to the closed conformation. Nevertheless, these interactions are not necessary for structuring of the C-terminal fragment, since this structuring occurs in the crystal structure of apo MorFDH in the absence of these interactions (at least in the case of the full-length form in the presence of sulfate). Therefore, the cofactor facilitates the transition of FDH to the closed form both directly and through the structuring of the C-terminal fragment 374–399.

The SAXS data for PseFDH show that apo PseFDH and the binary PseFDH–NAD^+ complex exist in the open conformation, in contrast to the triple PseFDH–NAD^+–azide complex. According to the SAXS results, the latter complex has a much more compact overall shape (Lamzin *et al.*, 1986). This is evidence that cofactor binding in itself is insufficient to cause such a substantial shift of the dynamic equilibrium in solution toward the closed conformation and that azide-ion binding is an important prerequisite for this transition. The substrate (formate ion) bears the same charge and can form the same hydrogen bonds as the azide ion. Hence, the substrate is presumably also important for the transition of the enzyme to the closed conformation necessary for catalysis. In our opinion, this hypothesis is supported by two considerations.

Firstly, binding of the negatively charged substrate/inhibitor compensates for the positive charge of the nicotinamide moiety of the cofactor and reduces the electrostatic repulsion between the positively charged nicotinamide ring and the guanidinium moiety of Arg284. The importance of electrostatic repulsion is confirmed by the fact that the binding of uncharged NADH is an order of magnitude stronger than that of NAD^+ (Popov & Lamzin, 1994).

Secondly, the azide ion in the catalytic site of MorFDH is bound to residues belonging to both the coenzyme-binding domain (Arg284 and His332) and the catalytic domain (Ile122 and Asn146) (Figs. 4 and 8). The structure of the binary PseFDH–formate complex shows that the formate ion is only bound to the catalytic domain residues Ile122 and Asn146 because the domains in the open conformation are spatially remote (Filippova *et al.*, 2006). The involvement of residues from both the catalytic and the coenzyme-binding domains in substrate/inhibitor binding in the closed conformation should assist in closure of the interdomain cleft.

4. Conclusions

MorFDH is structurally very similar to PseFDH, with the coenzyme-binding domain being more structurally conserved

than the catalytic domain. The catalytic properties of the recombinant full-length enzymes are also similar. However, a detailed comparison revealed a number of substantial differences. The MorFDH structures contain the extra C-terminal residues 392–399 compared with PseFDH. The dimer interface in the MorFDH molecule is characterized by a larger number of hydrogen bonds and salt bridges but a lower hydrophobicity. In the holo MorFDH structure the azide ion (a transition-state analogue) is involved in hydrogen bonding to the side chain of the catalytic residue His332. This fact supports the previous hypothesis that the catalytic residue His332 can form a hydrogen bond to both the substrate and the transition state, which contributes to the mechanism of the enzymatic reaction.

The most striking structural feature of apo MorFDH is that it has the closed conformation in the crystalline state, which is unique for an apo form of an NAD^+-dependent dehydrogenase. This is probably attributable to the presence of the extra C-terminal residues 392–399, sulfate-ion binding and the possible influence of the crystal contacts.

The MorFDH structures are very similar in both the presence and the absence of cofactor, except for differences in the adenine-binding subsite of the enzyme. Contrary to expectations, only the sulfate ion, one glycerol molecule and two additional water molecules were located in the cofactor-binding site. The adenine-binding subsite in the structure of the apo form is very labile, with some side-chain atoms in this region not being visible in electron-density maps. These facts indicate that the entropy factor plays a great role in coenzyme binding in FDH.

A comparison of bacterial FDH structures in the open and closed conformations shows that the change in the conformation of loop 221–226 in the adenine-binding subsite is greatly influenced by cofactor binding. In the absence of the cofactor this loop has the same conformation both in the open and closed forms. On the other hand, closure of the interdomain cleft results in the catalytic site residues becoming rigidly fixed in the catalytically competent conformation (in the open conformation these residues are spatially remote, the backbone of the loop Ile122–Asp125 has two conformations and the side chain of Arg284 adopts multiple conformations) and is accompanied by structuring of the C-terminal fragment 374–399 even without coenzyme binding.

The cofactor is an important prerequisite for the transition of the enzyme to the closed conformation because it acts as a bridge between the domains and facilitates the structuring of the C-terminal fragment 374–399, which forms additional interdomain interactions. Coenzyme binding influences the structuring of the C-terminal fragment both *via* hydrogen bonding and *via* a change in the conformation of loop 221–226, resulting in the latter also interacting with the C-terminal fragment. Furthermore, the conformational transition from the open to the closed form is facilitated by substrate/inhibitor binding, because it compensates for unfavourable electrostatic interactions within the enzyme active site and the substrate/inhibitor form bonds to residues from both the catalytic and the coenzyme-binding domains.

We thank Pavel Dorovatovskiy from the Kurchatov Center for Synchrotron Radiation and Nanotechnology and Alexey Nikulin from the Institute of Protein Research of the Russian Academy of Sciences for their kind support during the collection of X-ray data. The present study was financially supported by the Russian Federal Agency for Science and Innovations (Grant 02.512.12.2002) and the Russian Foundation for Basic Research (Project No. 08-04-00830-a).

References

Bandaria, J. N., Dutta, S., Hill, S. E., Kohen, A. & Cheatum, C. M. (2008). *J. Am. Chem. Soc.* **130**, 22–23.
Castillo, R., Oliva, M., Marti, S. & Moliner, V. (2008). *J. Phys. Chem. B*, **112**, 10012–10022.
Collaborative Computational Project, Number 4 (1994). *Acta Cryst.* D**50**, 760–763.
Emsley, P. & Cowtan, K. (2004). *Acta Cryst.* D**60**, 2126–2132.
Ernst, M., Kaup, B., Muller, M., Bringer-Meyer, S. & Sahm, H. (2005). *Appl. Microbiol. Biotechnol.* **66**, 629–634.
Filippova, E. V., Polyakov, K. M., Tikhonova, T. V., Stekhanova, T. N., Boiko, K. M. & Popov, V. O. (2005). *Crystallogr. Rep.* **50**, 796–800.
Filippova, E. V., Polyakov, K. M., Tikhonova, T. V., Stekhanova, T. N., Boiko, K. M., Sadykhov, I. G., Tishkov, V. I. & Popov, V. O. (2006). *Crystallogr. Rep.* **51**, 627–631.
Folch, B., Rooman, M. & Dehouck, Y. (2007). *J. Chem. Inf. Model.* **48**, 119–127.
Hayward, S. & Kitao, A. (2006). *Biophys. J.* **91**, 1823–1831.
Kabsch, W. (1993). *J. Appl. Cryst.* **26**, 795–800.
Kabsch, W. & Sander, C. (1983). *Biopolymers*, **22**, 2577–2637.
Klein, C. & Bartels, K. S. (2000). *Acta Cryst.* A**56**, s295.
Krissinel, E. & Henrick, K. (2007). *J. Mol. Biol.* **372**, 774–797.
Kumar, S., Ma, B., Tsai, C. J., Wolfson, H. & Nussinov, R. (1999). *Cell Biochem. Biophys.* **31**, 141–164.
Lamzin, V. S., Asadchikov, V. E., Popov, V. O., Egorov, A. M. & Berezin, I. V. (1986). *Dokl. Akad. Nauk SSSR*, **291**, 1011–1014.
Lamzin, V. S., Dauter, Z., Popov, V. O., Harutyunyan, E. H. & Wilson, K. S. (1994). *J. Mol. Biol.* **236**, 759–785.
Larkin, M. A., Blackshields, G., Brown, N. P., Chenna, R., McGettigan, P. A., McWilliam, H., Valentin, F., Wallace, I. M., Wilm, A., Lopez, R., Thompson, J. D., Gibson, T. J. & Higgins, D. G. (2007). *Bioinformatics*, **23**, 2947–2948.
Laskowski, R. A., MacArthur, M. W., Moss, D. S. & Thornton, J. M. (1993). *J. Appl. Cryst.* **26**, 283–291.
Li, W. F., Zhou, X. X. & Lu, P. (2005). *Biotechnol. Adv.* **23**, 271–281.
Murshudov, G. N., Vagin, A. A. & Dodson, E. J. (1997). *Acta Cryst.* D**53**, 240–255.
Popov, V. O. & Lamzin, V. S. (1994). *Biochem. J.* **301**, 625–643.
Popov, V. O. & Tishkov, V. I. (2003). *Protein Structures: Kaleidoscope of Structural Properties and Functions*, edited by V. N. Uversky, pp. 441–473. Kerala, India: Research Signpost.
Potterton, L., McNicholas, S., Krissinel, E., Gruber, J., Cowtan, K., Emsley, P., Murshudov, G. N., Cohen, S., Perrakis, A. & Noble, M. (2004). *Acta Cryst.* D**60**, 2288–2294.
Razeto, A., Kochhar, S., Hottinger, H., Dauter, M., Wilson, K. S. & Lamzin, V. S. (2002). *J. Mol. Biol.* **318**, 109–119.
Sadykhov, E. G., Serov, A. E., Voinova, N. S., Uglanova, S. V., Petrov, A. S., Alekseeva, A. A., Kleimenov, S. I., Popov, V. I. & Tishkov, V. I. (2006). *Prikl. Biokhim. Mikrobiol.* **42**, 269–273.
Schirwitz, K., Schmidt, A. & Lamzin, V. S. (2007). *Protein Sci.* **16**, 1146–1156.
Stillman, T. J., Migueis, A. M., Wang, X. G., Baker, P. J., Britton, K. L., Engel, P. C. & Rice, D. W. (1999). *J. Mol. Biol.* **285**, 875–885.
Tishkov, V. I. (2009). Personal communication.
Tishkov, V. I., Galkin, A. G. & Egorov, A. M. (1991). *Dokl. Akad. Nauk SSSR*, **317**, 745–748.

Tishkov, V. I., Galkin, A. G., Fedorchuk, V. V., Savitsky, P. A., Rojkova, A. M., Gieren, H. & Kula, M. R. (1999). *Biotechnol. Bioeng.* **64**, 187–193.
Tishkov, V. I., Matorin, A. D., Rojkova, A. M., Fedorchuk, V. V., Savitsky, P. A., Dementieva, L. A., Lamzin, V. S., Mezentzev, A. V. & Popov, V. O. (1996). *FEBS Lett.* **390**, 104–108.
Tishkov, V. I. & Popov, V. O. (2004). *Biochemistry (Mosc.)*, **69**, 1252–1267.
Tishkov, V. I. & Popov, V. O. (2006). *Biomol. Eng.* **23**, 89–110.
Torres, R. A., Schitt, B. & Bruice, T. C. (1999). *J. Am. Chem. Soc.* **121**, 8164–8173.
Vagin, A. & Teplyakov, A. (1997). *J. Appl. Cryst.* **30**, 1022–1025.
Vinals, C., Depiereux, E. & Feytmans, E. (1993). *Biochem. Biophys. Res. Commun.* **192**, 182–188.
Weckbecker, A. & Hummel, W. (2004). *Biotechnol. Lett.* **26**, 1739–1744.